CONF-9504 20--19

ERROR ANALYSIS OF THE QUARTIC NODAL EXPANSION METHOD FOR SLAB GEOMETRY*

R. C. Penland[a]
Y. Y. Azmy[b]
P. J. Turinsky[a]

[a]North Carolina State University
P.O. Box 7909
Raleigh, North Carolina 27695

[b]Oak Ridge National Laboratory
Engineering Physics and Mathematics Division
P.O. Box 2008, Bldg. 6025
Oak Ridge, Tennessee 37831-6363

Full paper for presentation to the *International Conference on Mathematics and Computations, Reactor Physics, and Environmental Analyses*, April 30–May 4, 1995, Portland, Oregon.

*Research sponsored by the U.S. Department of Energy under contract No. DE-AC05-84OR21400 with Martin Marietta Energy Systems, Inc.

PWR

ERROR ANALYSIS OF THE QUARTIC NODAL EXPANSION METHOD FOR SLAB GEOMETRY

R. C. Penland[a]
Y. Y. Azmy[b]
P. J. Turinsky[a]

[a] North Carolina State University, P.O. Box 7909, Raleigh, NC, 27695, USA
TEL: (919)515-2301, E-mail: rcpenlan@eos.ncsu.edu, turinsky@eos.ncsu.edu

[b] Oak Ridge National Laboratory, P.O. Box 2008, Oak Ridge, TN, 37831-6363, USA
TEL:(615)574-8069, E-mail: yya@ornl.gov

KEYWORDS: Error Analysis, Nodal Expansion Method

ABSTRACT

This paper presents an analysis of the quartic polynomial Nodal Expansion Method (NEM) for one-dimensional neutron diffusion calculations. As part of an ongoing effort to develop an adaptive mesh refinement strategy for use in state-of-the-art nodal kinetics codes, we derive *a priori* error bounds on the computed solution for uniform meshes and validate them using a simple test problem. Predicted error bounds are found to be greater than computed maximum absolute errors by no more than a factor of six allowing mesh size selection to reflect desired accuracy. We also quantify the rapid convergence in the NEM computed solution as a function of mesh size.

I. INTRODUCTION

The next logical advancement in the solution of the neutron diffusion equation is the development of an adaptive mesh refinement strategy for nodal methods. The ability would then exist to solve problems with locallized, transient phenomena to a desired degree of accuracy without having to experimentally customize the solution mesh. The major requirement for such an undertaking is that we have an efficient means of estimating the error in the computed solution so that we may identify areas needing mesh refinement. At North Carolina State University, there is continuing effort to construct a modern nodal kinetics code.[1] The NESTLE code, as it is called, is the target for the aforementioned adaptive mesh refinement scheme.

Using the traditional variable nomenclature where L is the neutron diffusion length, D is the diffusion coeffcient and s(x) is the spatial distribution of the neutron source, the one group neutron diffusion equation in homogeneous slab geometry is given by,

$$\frac{d^2}{dx^2}\phi(x) - \frac{1}{L^2}\phi(x) = \frac{s(x)}{D} \tag{1}$$

Application of the Nodal Expansion Method (NEM) to neutron diffusion calculations in slab geometry is based on the assumption that the neutron flux as a function of position within node $i = 1, \ldots, N$ can be projected accurately on a set of polynomial basis functions, specifically

$$\phi^i(x) = \sum_{k=0}^{4} a_k^i f_k(x) \tag{2}$$

The basis functions we choose are those developed by Finnemann, et al.,[2] defined on the normalized spatial interval [-1/2, 1/2] corresponding to the node shifted interval $[-\frac{\Delta x}{2}, \frac{\Delta x}{2}]$ and absolute interval $[x_{i-1}, x_i]$. Traditionally, the discrete variables to be computed are the basis function coefficients, but we find it convenient to use the more physical surface fluxes and flux moments within a cell instead. Let $\bar{\phi}_m^i$ denote the flux moment resulting from weighting the

flux distribution in the i^{th} node with the m^{th} basis function, and denote ϕ^i_+ and ϕ^i_- to be the flux on the east and west surfaces of node i respectively. The results of this tranformation are given here,

$$\begin{aligned} a^i_0 &= \bar{\phi}^i_0 \\ a^i_1 &= \phi^i_+ - \phi^i_- \\ a^i_2 &= \phi^i_+ - 2\bar{\phi}^i_0 + \phi^i_- \\ a^i_3 &= 10\phi^i_+ - 10\phi^i_- - 120\bar{\phi}^i_1 \\ a^i_4 &= 35\phi^i_+ - 70\bar{\phi}^i_0 - 700\bar{\phi}^i_2 + 35\phi^i_- \end{aligned} \tag{3}$$

The following "moment equations" are the constraints that arise from weighting the neutron diffusion equation with the first three basis functions,

$$\frac{20\phi^i_+ - 40\bar{\phi}^i_0 - 280\bar{\phi}^i_2 + 20\phi^i_-}{\Delta x^2} - \frac{\bar{\phi}^i_0}{L^2} = -\frac{\bar{s}^i_0}{D} \tag{4}$$

$$\frac{5\phi^i_+ - 60\bar{\phi}^i_1 - 5\phi^i_-}{\Delta x^2} - \frac{\bar{\phi}^i_1}{L^2} = -\frac{\bar{s}^i_1}{D} \tag{5}$$

$$\frac{7\phi^i_+ - 14\bar{\phi}^i_0 - 140\bar{\phi}^i_2 + 7\phi^i_-}{\Delta x^2} - \frac{\bar{\phi}^i_2}{L^2} = -\frac{\bar{s}^i_2}{D} \tag{6}$$

Additional equations result from enforcing current continuity accross cell boundaries,

$$\begin{aligned} &\frac{D^i}{\Delta x}\left[4\phi^i_- - 20\bar{\phi}^i_0 - 60\bar{\phi}^i_1 - 140\bar{\phi}^i_2 + 16\phi^i_+\right] = \\ &\frac{D^{i+1}}{\Delta x}\left[-16\phi^{i+1}_- + 20\bar{\phi}^{i+1}_0 - 60\bar{\phi}^{i+1}_1 + 140\bar{\phi}^{i+1}_2 - 4\phi^{i+1}_+\right] \end{aligned} \tag{7}$$

Numerical studies have supported the use of this procedure as a valid source of closure equations in high-order NEM[2]. Flux continuity at these same interfaces is also imposed. The final two equations necessary to close the system are given by Dirichlet boundary conditions, $\phi^1_- = \phi^N_+ = 0$ in our study.

II. ERROR ANALYSIS

A. Uniqueness of Solution

The methodology employed in the error analysis of the quartic NEM equations parallels that presented by Ortega for finite difference methods.[3] We derive a "Maximum Principle" to show that the problem solution is unique, a property necessary if we are to bound the truncation error. We first use flux continuity across cell boundaries to reduce the number of unknowns by one-fifth. The notation will now reflect that ϕ^i is the flux at the surface located at x_i on the east boundary of node i. Furthermore, we assume homogeneous nuclear properties and choose to work only with a uniform mesh.

Hypothesize that the set $\{\bar{\phi}^i_m, \phi^i\}, m = 0, 1, 2$ is not a unique solution to the discrete problem and that there is a second solution that we will call $\{\bar{\psi}^i_m, \psi^i\}, m = 0, 1, 2$. If we now form the difference of the moment equations and continuity equations, we develop an analogous problem for the unknowns $\bar{\xi}^i_m = \bar{\phi}^i_m - \bar{\psi}^i_m$ and $\xi^i = \phi^i - \psi^i$ given by,

$$20\xi^i - \left[40 + \frac{\Delta x^2}{L^2}\right]\bar{\xi}^i_0 - 280\bar{\xi}^i_2 + 20\xi^{i-1} = 0 \tag{8}$$

$$5\xi^i - \left[60 + \frac{\Delta x^2}{L^2}\right]\bar{\xi}^i_1 - 5\xi_{i-1} = 0 \tag{9}$$

$$7\xi^i - 14\bar{\xi}^i_0 - \left[140 + \frac{\Delta x^2}{L^2}\right]\bar{\xi}^i_2 + 7\xi^{i-1} = 0 \tag{10}$$

$$4\xi^{i-1} - 20\bar{\xi}_0^i - 60\bar{\xi}_1^i - 140\bar{\xi}_2^i + 32\xi^i - 140\bar{\xi}_2^{i+1} + 60\bar{\xi}_1^{i+1} - 20\bar{\xi}_0^{i+1} + 4\xi^{i+1} = 0 \tag{11}$$

Note that the new problem is homogeneous regardless of the original conditions. Also, the solution of these equations is subject to Dirichlet boundary conditions. Solution of (9) for the variable $\bar{\xi}_1^i$ followed by application of the Triangle Inequality[4] reveals,

$$|\bar{\xi}_1^i| \leq |\alpha|(|\xi^i| + |\xi^{i-1}|) \quad where \quad \alpha = \frac{5}{60 + \frac{\Delta x^2}{L^2}} \tag{12}$$

From the definition of α, it can be seen that it is always positive and $|\alpha| \leq \frac{1}{2}$. Such properties guarantee that $|\bar{\xi}_1^i| \leq max\{|\xi^i|, |\xi^{i-1}|\}$. The maximum value of $|\xi|$ therefore cannot occur in the variable $\bar{\xi}_1^i$. Solving (10) for $\bar{\xi}_2^i$ and substituting into (8), we are able to apply the Triangle Inequality once again to arrive at,

$$|\bar{\xi}_0^i| \leq |\beta|(|\xi^i| + |\xi^{i-1}|) \quad where \quad \beta = \frac{3 + \frac{\Delta x^2}{14L^2}}{6 + \frac{9\Delta x^2}{14L^2} + \frac{\Delta x^4}{280L^2}} \tag{13}$$

Examination of β shows it to have attributes identical to those of α defined previously. We then conclude that the maximum value of $|\xi|$ is not taken by the variable $\bar{\xi}_0^i$. Conversely, isolating $\bar{\xi}_0^i$ in (8) for substitution into (10) results in, after use of the Triangle Inequality,

$$|\bar{\xi}_2^i| \leq |\gamma|(|\xi^i| + |\xi^{i-1}|) \quad where \quad \gamma = \frac{7\frac{\Delta x^2}{L^2}}{1680 + 180\frac{\Delta x^2}{L^2} + \frac{\Delta x^4}{L^4}} \tag{14}$$

As before, properties of γ do not allow the maximum value of $|\xi|$ to occur in $\bar{\xi}_2^i$. Therefore, the maximum absolute difference must occur at a cell boundary.

Using the moment equations, we eliminate variables in (11) leaving only the surface quantities. Following considerable manipulation and application of the Triangle Inequality, we obtain

$$|\xi^i| \leq |\eta|(|\xi^{i+1}| + |\xi^{i-1}|) \quad where \quad \eta = \frac{100800 - 4320\frac{\Delta x^2}{L^2} + 120\frac{\Delta x^4}{L^4} - 4\frac{\Delta x^6}{L^6}}{2217600 + 308160\frac{\Delta x^2}{L^2} + 4980\frac{\Delta x^4}{L^4} + 32\frac{\Delta x^6}{L^6}} \tag{15}$$

Note that $|\eta| \leq \frac{1}{2}$ and $\eta \geq 0$ for $\Delta x \leq 5L$, a condition that must be satisfied in the limit $\Delta x \to 0$ that is necessary for the error analysis. Assume there is a maximum value in $|\xi^i|$ and let it occur at the surface x_k. Furthermore, let $|\xi^{k+1}| \geq |\xi^{k-1}|$ allowing replacement of the latter by the former in (15) and using the properties of η we conclude,

$$|\xi^k| \leq 2|\eta|\ |\xi^{k+1}| \leq |\xi^{k+1}| \tag{16}$$

The only statement that can satisfy both this equation and the claim made on $|\xi^k|$ as a maximum is that $|\xi^k| = |\xi^{k+1}|$. Similar logic applied to the alternative option $|\xi^{k+1}| \leq |\xi^{k-1}|$ yields the result that,

$$|\xi^k| = max\left\{|\xi^{k+1}|, |\xi^{k-1}|\right\} \tag{17}$$

Using this information in (15) leads us to the important result,

$$|\xi^{k-1}| = |\xi^k| = |\xi^{k+1}| \tag{18}$$

We conclude that if a maximum does in fact occur in the interior of the region then $|\xi|$ is constant everywhere within the region. A more general statement of this is that the maximum of $|\xi|$ must occur on the boundaries of the region. Recall the boundary conditions set $\xi^0 = \xi^N = 0$. Therefore, $\xi^i = \bar{\xi}_m^i = 0$; $m = 0, 1, 2$; $i = 1 \ldots N$ implying that the solution of the original problem is unique.

B. Error Bounds

Turning now to the question of bounding the error in the solution, denote the exact flux solution quantities by Φ so that we may define the error in the solution as, $e^i = \phi^i - \Phi^i$, $\bar{e}_m^i = \bar{\phi}_m^i - \bar{\Phi}_m^i$ for each cell i and moment indices $m = 0, 1, 2$. Starting with the zero moment equation, (4), and subtracting from each side the following expression,

$$20\Phi^i - \left[40 + \frac{\Delta x^2}{L^2}\right]\bar{\Phi}_0^i - 280\bar{\Phi}_2^i + 20\Phi^{i-1} \tag{19}$$

we arrive at the expression,

$$-20e^i + \left[40 + \frac{\Delta x^2}{L^2}\right]\bar{e}_0^i + 280\bar{e}_2^i - 20e^{i-1} = \Delta x^2 \tau_0(i,\Delta x) \tag{20}$$

where we have defined the zero moment discretization error to be,

$$\tau_0(i,\Delta x) \equiv \frac{20\Phi^i - \left[40 + \frac{\Delta x^2}{L^2}\right]\bar{\Phi}_0^i - 280\bar{\Phi}_2^i + 20\Phi^{i-1}}{\Delta x^2} - \frac{1}{\Delta x}\int_{x_{i-1}}^{x_i} \frac{d^2\Phi}{dx^2}dx \tag{21}$$

This form arises from substitution of the source term in terms of the exact flux. Similarly, subtraction of the expression,

$$5\Phi^i - \left[60 + \frac{\Delta x^2}{L^2}\right]\bar{\Phi}_1^i - 5\Phi^{i-1} \tag{22}$$

from each side of the first moment equation, (5), leads to the form,

$$-5e^i + \left[60 + \frac{\Delta x^2}{L^2}\right]\bar{e}_1^i = \Delta x^2 \tau_1(i,\Delta x) \tag{23}$$

with an analogous definition of the first moment discretization error,

$$\tau_1(i,\Delta x) \equiv \frac{5\Phi^i - 60\bar{\Phi}_1^i - 5\Phi^{i-1}}{\Delta x^2} - \frac{1}{\Delta x}\int_{x_{i-1}}^{x_i} f_1(x)\frac{d^2\Phi}{dx^2}dx \tag{24}$$

Treatment of the second moment equations, (6), and current continuity equation, (7), are natural extensions leading to the forms,

$$-7e^i + 14\bar{e}_0^i + \left[140 + \frac{\Delta x^2}{L^2}\right]\bar{e}_2^i - 7e^{i-1} = \Delta x^2 \tau_2(i,\Delta x) \tag{25}$$

$$-4e^{i-1} + 20\bar{e}_0^i + 60\bar{e}_1^i + 140\bar{e}_2^i - 32e^i + 140\bar{e}_2^{i+1} - 60\bar{e}_1^{i+1} + 20\bar{e}_0^{i+1} - 4e^{i+1} = \Delta x \tau_c(i,\Delta x) \tag{26}$$

where the corresponding discretization errors are defined by,

$$\tau_2(i,\Delta x) \equiv \frac{7\Phi^i - 14\bar{\Phi}_0^i - 140\bar{\Phi}_2^i + 7\Phi^{i-1}}{\Delta x^2} - \frac{1}{\Delta x}\int_{x_{i-1}}^{x_i} f_2(x)\frac{d^2\Phi}{dx^2}dx \tag{27}$$

$$\tau_c(i,\Delta x) \equiv \frac{4}{\Delta x}[(\Phi^{i-1} + \Phi^{i+1}) - 5(\bar{\Phi}_0^i + \bar{\Phi}_0^{i+1}) - 12(\bar{\Phi}_1^i - \bar{\Phi}_1^{i+1}) - 35(\bar{\Phi}_2^i + \bar{\Phi}_2^{i+1}) + 8\Phi^i] \tag{28}$$

These expressions indicate that the errors introduced are given by the differences of derivatives in the exact equations with difference forms in the discrete variable equations.

We now try to show that the truncation errors in the discrete variables are in some way bounded by a combination of the different discretization errors. First isolate the cell moment variables in terms of surface variables and discretization errors using the moment-type equations. A bound on the surface flux error is then found and used to extract error bounds for the cell moment quantities. We solve for $\bar{e}_2^i$ from (25) and substitute into (20) to isolate $\bar{e}_0^i$. The result is shown here,

$$\bar{e}_0^i = \frac{\left(840 + \frac{20\Delta x^2}{L^2}\right)(e^i + e^{i-1}) + \left(140 + \frac{\Delta x^2}{L^2}\right)\Delta x^2 \tau_0(i,\Delta x) - 280\Delta x^2 \tau_2(i,\Delta x)}{1680 + 180\frac{\Delta x^2}{L^2} + \frac{\Delta x^4}{L^4}} \tag{29}$$

Isolation of $\bar{e}_2^i$ is accomplished by solving (20) for $\bar{e}_0^i$ and inserting this result into (25) to obtain,

$$\bar{e}_2^i = \frac{\frac{7\Delta x^2}{L^2}(e^i + e^{i-1}) + \left(40 + \frac{\Delta x^2}{L^2}\right)\Delta x^2 \tau_2(i,\Delta x) - 14\Delta x^2 \tau_0(i,\Delta x)}{1680 + 180\frac{\Delta x^2}{L^2} + \frac{\Delta x^4}{L^4}} \tag{30}$$

The solution of (23) for $\bar{e}_1^i$ is straightforward resulting in,

$$\bar{e}_1^i = \frac{1}{60 + \frac{\Delta x^2}{L^2}} \left[5(e^i - e^{i-1}) + \Delta x^2 \tau_1(i, \Delta x)\right] \tag{31}$$

Finally, these expressions are used in (26) to obtain an error bound for $|e^i|$, a long and tedious process which we will refrain from showing here.

The properties of the local discretization error now warrant further investigation. The most important property to establish is that the discretization errors approach zero in the limit as $\Delta x \rightarrow 0$ since this guarantees the truncation error will also approach zero. We will also determine in the case that the exact flux solution is sufficiently smooth the rate at which the local discretization error components approach zero. This allows us to write a Taylor series expansion for the exact flux about the surface at x_i. This is done to simplify the combination of discretization error components in the expression for e^i. Without assuming the exact flux solution is sufficiently smooth to allow expansion to high order, the following exercise terminates with the realization that the discretization error goes to zero but at an unknown rate.

It is important to note an implicit variable translation when weighting the Taylor series expansion of the flux using the basis functions, as required to evaluate the local discretization errors. The basis functions were intended to be used on the interval $[\frac{-\Delta x}{2}, \frac{\Delta x}{2}]$, so there is a "shifting" that must occur to use the interval $[0, \Delta x]$ when we center the Taylor series expansion on the surface x_i. For clarity, a superscript is introduced on the basis function to indicate the cell in which the basis function is used. Since the zero order basis function is a constant, the shift is inconsequential but becomes important in higher order basis functions as shown here,

$$\begin{aligned} f_1^i(x) &= \frac{x + \frac{\Delta x}{2}}{\Delta x} & f_1^{i+1}(x) &= \frac{x - \frac{\Delta x}{2}}{\Delta x} \\ f_2^i(x) &= 3\left(\frac{x + \frac{\Delta x}{2}}{\Delta x}\right)^2 - \frac{1}{4} & f_2^{i+1}(x) &= 3\left(\frac{x - \frac{\Delta x}{2}}{\Delta x}\right)^2 - \frac{1}{4} \end{aligned} \tag{32}$$

Combining all these terms into (21) for nodes i and $i+1$ promotes significant cancellation. Application of the Triangle Inequality to the expression derived for e^i results in,

$$|e^i| \leq \frac{(201600 - 8640\frac{\Delta x^2}{L^2} + 240\frac{\Delta x^4}{L^4} - 8\frac{\Delta x^6}{L^6})|e| + \frac{4M^{(vi)}\Delta x^8}{9L^2}}{201600 + 92160\frac{\Delta x^2}{L^2} + 4320\frac{\Delta x^4}{L^4} + 32\frac{\Delta x^6}{L^6}} \tag{33}$$

where we have replaced $|e^{i-1}|$ and $|e^{i+1}|$ by the maximum surface flux error denoted $|e|$. $M^{(n)}$ implies the maximum absolute value of the n^{th} exact flux derivative over the Taylor series expansion points. Terms of order greater than six have been neglected since this analysis focuses on asymptotic error behavior. This expression is true for all nodes, including the node where the maximum is actually attained. The coefficient of $|e|$ can take on either arithmetic sign depending on the value of Δx. We will only examine the case where this coefficient is positive, $\Delta x^2 \leq 5L^2$ since this is true in the limit of small Δx. Evaluating (33) at the location of the maximum, we solve for the maximum surface flux error bound as,

$$|e| \leq \frac{M^{(vi)}\Delta x^6}{226800} \tag{34}$$

We apply the Triangle Inequality to (29) to obtain,

$$|\bar{e}_0^i| \leq \frac{\left(840 + \frac{20\Delta x^2}{L^2}\right)(|e^i| + |e^{i-1}|) + \frac{M^{(vi)}\Delta x^6}{54}}{1680 + 180\frac{\Delta x^2}{L^2} + \frac{\Delta x^4}{L^4}} \tag{35}$$

We now derive a bound on $|\bar{e}_0^i|$ by replacing $|e^i|$ and $|e^{i+1}|$ with the upper bound given by (34),

$$\therefore \quad |\bar{e}_0| \leq \frac{M^{(vi)}\Delta x^6}{64800} \tag{36}$$

where $|\bar{e}_0|$ represents the maximum absolute error in the zero flux moment. Extension of this treatment to the other cell moment errors isolated in (31) and (30) yields similar results,

$$|\bar{e}_1| \leq \frac{M^{(v)}\Delta x^5}{100800} \tag{37}$$

$$|\bar{e}_2| \leq \frac{17M^{(vi)}\Delta x^6}{12700800} \tag{38}$$

Summarizing the analysis, we conclude that the error quantities $|e|$, $|\bar{e}_0|$, and $|\bar{e}_2|$ behave as Δx^6 while the error $|\bar{e}_1|$ is order Δx^5.

We now discuss how these results can be used within the context of adaptive mesh refinement. Our goal is to develop an error estimation technique based on information generated during multilevel acceleration cycles. This implies that we wish to relate the infinity norm of the error incurred at mesh level N to the expression $|\phi(N)-\phi^R(N)|$. The term $\phi(N)$ is any of the computed unknowns on mesh level N and $\phi^R(N)$ is the same unknown at mesh level N reconstructed from the solution at mesh level $2N$. It should be clear that the following equality holds.

$$\|\phi(N) - \phi^R(N)\|_\infty = \|e(N) - e^R(N)\|_\infty \tag{39}$$

Application of the Triangle Inequality and assumption that the infinity norm of each error variable behaves as $C\Delta x^p$ where p is known leads us to a relationship for C.

$$C \leq \frac{2^p\|\phi(N) - \phi^R(N)\|_\infty}{(1+2^p)\Delta x^p(N)} \tag{40}$$

Performing the NEM solution on mesh levels N and $2N$ permits calculation of the upperbounding value of this coefficient, which can subsequently be used to predict the mesh size that is necessary to satisfy a desired error tolerance in each variable. This provides a basis for adaptive mesh refinement.

III. VALIDATION

The simple test problem considered for this analysis consists of a one-dimensional slab $[0, a]$ with uniform nuclear properties. The slab has a unit source distributed uniformly throughout. Only one energy group will be treated since we seek a simple analytic solution used to find the error incurred by solving the problem with the NEM approximation. The system chosen for the test problem was a 0.20m thick water slab with $D = 1.429 \times 10^{-3}m$ and $\Sigma_a = 2.2m^{-1}$. Behavior of the solution in a graphite medium was found qualitatively no different.

A computer program was developed to solve the equations resulting from the NEM formulation. The algebraic system was cast in matrix form $\mathbf{Ax} = \mathbf{b}$ and solved in double precision using established LU factorization (DGECO) and solver (DGESL) routines from the LINPACK library.[5] Estimates of the inverse of the matrix condition number are calculated to warn of potential roundoff problems in the solution when the number of nodes, hence the matrix dimension, becomes large.

The largest problem size possible is dictated by the size of memory available on the computer and is compounded by the fact that we are forced to work in double precision lest the roundoff errors become intolerable at small numbers of nodes well before asymptotic error behavior is observed. Summarily, the condition number of the coefficient matrix became intolerable in advance of the memory constraint. Erratic, oscillatory values contaminated the solution vector and destroyed the monotonicity of the error behavior.

We calculate an asymptotic error order by assuming the infinity norm of all variables behave like $C\Delta x^p$. Therefore, we compare maximum absolute error on mesh N and on mesh $2N$ to determine the value of p independent of the leading coefficient.

$$\frac{|e|^{2N}_{max}}{|e|^{N}_{max}} \approx \frac{C\left[\frac{\Delta x}{2}\right]^p}{C\Delta x^p} \approx 2^{-p} \tag{41}$$

IV. CONCLUSIONS

As a first step in verifying our analysis, it is important that the asymptotic error order for each discrete variable is consistent between the analysis and experiment. Table 1 clearly shows this to be the case. The error order for the zero flux moment seemingly decreases in the final trial, but recall the fact that we are solving the system of equations on a finite precision computer. The drop in error order is attributable to roundoff contamination of our solution. Note that the error order for the first flux moment tends to approach its theoretical limit much slower than the other variables, which will be explained below.

The attached figures compare the analytic error bound in each variable with the computed data for the discrete variables in the quartic NEM. The computed maximum absolute errors for flux moments zero and two are approximately six times smaller than those estimated by the analysis evidenced by Figure 2 and Figure 4. The computed maximum absolute surface flux error in Figure 1 is observed to violate the analytic error bound at very coarse meshes. The computed value of $|\bar{e}_1^i|$ violates its analytic error bound over most mesh sizes shown in Figure 3. Wee believe that the bound violations noted can be explained by looking at the terms truncated in the analytic error bounds we derived. For each of the even flux moments, the neglected term was $O(\Delta x^8)$, two orders higher than the leading term. The same is true for the surface flux error bound, but the coefficient of the $O(\Delta x^8)$ term relative to the coefficient of the $O(\Delta x^6)$ term is larger for the the surface flux error versus the even flux moment errors. The term ignored in the first flux moment error bound is only $O(\Delta x^6)$, one order higher than the leading term. In each case, the truncated terms are additive and tend to raise the bound. Moreover, Table 1 supports the observation that the first flux moment is the last to reach asymptotic error behavior. The effect of these truncated terms on error bound violations and error order convergence is still subject to further research.

Results of our attempt to predict the appropriate mesh needed to satisfy a given tolerance are given in Table 2. During this phase of our work, it was noted that doubling the mesh for quartic NEM so greatly improves the fidelity of the solution that it effectively reproduces the exact solution on the coarser mesh. The implication is that (40) provides the value of C versus an upper bounding value since we assume that both reconstructed and non-reconstructed variables behave in a similar way. Such behavior is very useful when performing error estimation in the context of multilevel acceleration.

Work is underway investigating the effects of non-Dirichlet boundary conditions and material heterogeneities when deriving bounds as we have done. Future efforts will center on application of this method to multi-dimensional geometries.

ACKNOWLEDGEMENTS

This work was supported in part by the Computational Science Graduate Fellowship Program of the Office of Scientific Computing in the Department of Energy.

Mesh Spacing Coarse - Fine (10^{-2}m)	Asymptotic Error Order $\|e^i\|$	$\|\vec{e}_0^i\|$	$\|\vec{e}_1^i\|$	$\|\vec{e}_2^i\|$
$5.00 - 2.50$	5.8	5.3	4.2	5.5
$2.50 - 1.25$	6.0	5.8	4.6	5.7
$1.25 - 0.625$	6.0	6.0	4.8	5.8
$0.625 - 0.3125$	6.0	5.7	4.9	6.0

Table 1: Computed asymptotic order of the error for the discrete variables for the quartic NEM solution to the test problem on various uniform meshes.

Tolerance on $\|\vec{e}_0^i\|$	Predicted Mesh Number	Computed $\|\vec{e}_0^i\|$
10^{-3}	4	1.27×10^{-4}
10^{-5}	8	3.22×10^{-6}
10^{-7}	16	5.61×10^{-8}
10^{-9}	32	9.06×10^{-10}

Table 2: Results of mesh size prediction using fine to coarse mesh reconstruction as a basis for error estimation.

REFERENCES

1. P. J. TURINSKY, R. M. AL-CHALABI, P. ENGRAND, H. N. SARSOUR, F. X. FAURE, W. GUO, *NESTLE: Few-Group Neutron Diffusion Equation Solver Utilizing Nodal Expansion Method for Eigenvalue, Adjoint, Fixed-Source, Steady-State and Transient Problems*, EGG-NRE-11406 (1994).
2. H. FINNEMANN et al., "Interface Current Techniques for Multidimensional Reactor Calculations", *Atomkerenergie*, **30**, 123 (1977).
3. J. ORTEGA, *Numerical Analysis: A Second Course*, SIAM: Philadelphia (1990).
4. R. G. BARTLE, *The Elements of Real Analysis*, 2nd ed., John Wiley & Sons, New York (1976).
5. J. J. DONGARRA, J. R. BUNCH, C. B. MOLER, AND G. W. STEWART, *LINPACK Users' Guide*, SIAM, Philadelphia, PA (1979).

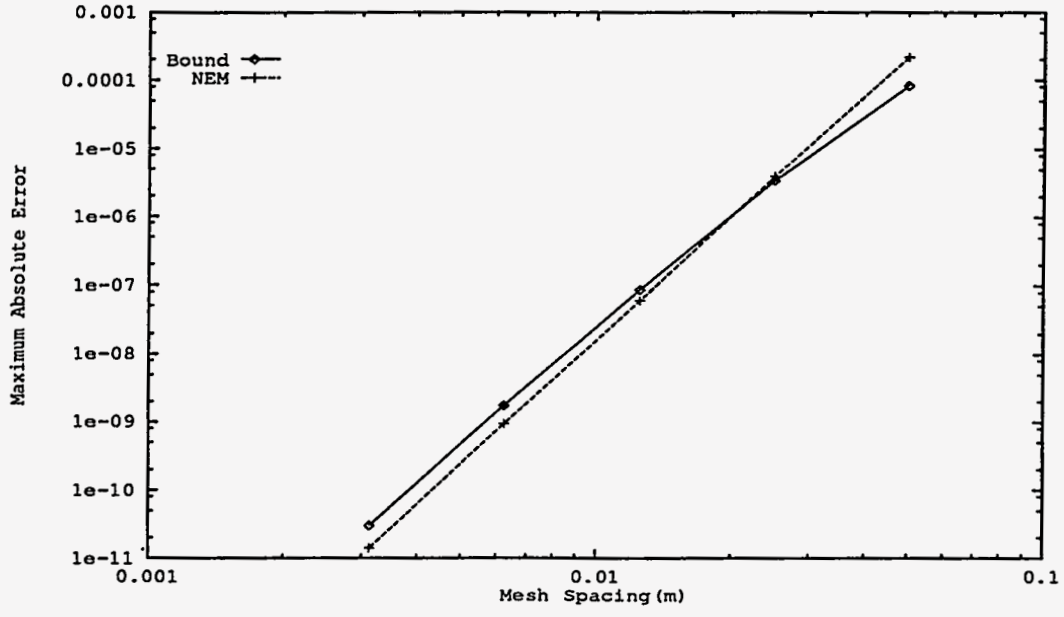

Figure 1: Comparison of the computed maximum and the derived upper bound on the surface flux absolute error ($|e^i|$) for the quartic NEM solution to the test problem on various uniform meshes.

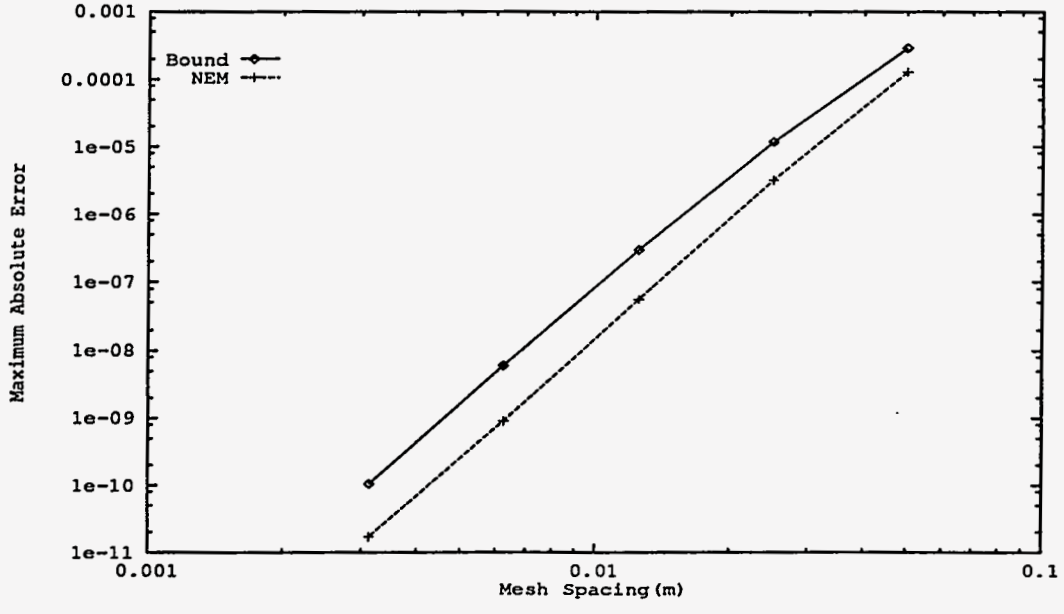

Figure 2: Comparison of the computed maximum and the derived upper bound on the zeroth flux moment absolute error ($|\bar{e}_0^i|$) for the quartic NEM solution to the test problem on various uniform meshes.

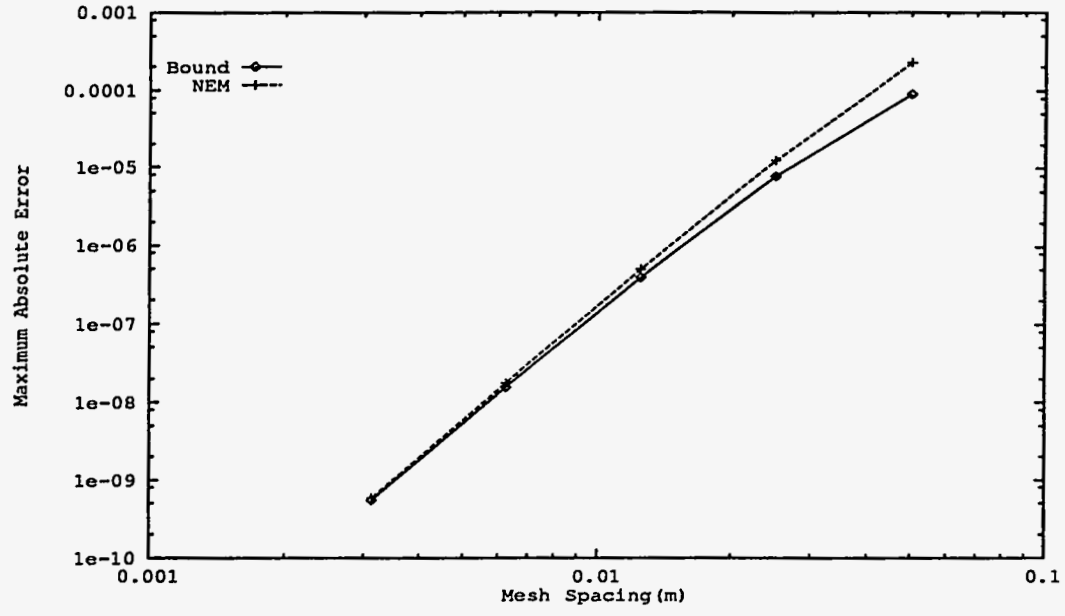

Figure 3: Comparison of the computed maximum and the derived upper bound on the first flux moment absolute error ($|\vec{e}_1^i|$) for the quartic NEM solution to the test problem on various uniform meshes.

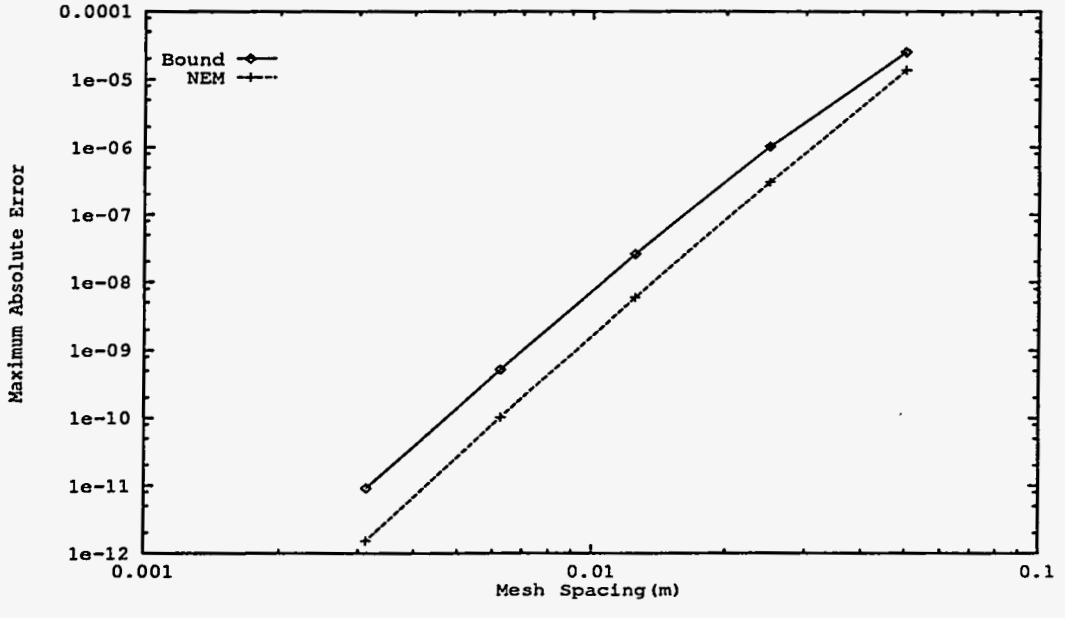

Figure 4: Comparison of the computed maximum and the derived upper bound on the second flux moment absolute error ($|\vec{e}_2^i|$) for the quartic NEM solution to the test problem on various uniform meshes.